

**Flow coefficients in O-O, Al-Al, and Cu-Cu collisions at 200 GeV in the fusing color string model**M. A. Braun<sup>1</sup> and C. Pajares<sup>2</sup><sup>1</sup>*Department of High Energy Physics, Saint-Petersburg State University, Russia*<sup>2</sup>*Department of Particles and Instituto Gallego de Altas Energias, University of Santiago de Compostela, Spain*

(Received 23 September 2020; revised 12 April 2021; accepted 19 April 2021; published 5 May 2021)

In view of the planning experiments for collisions of light nuclei at relativistic heavy ion collider, the flow coefficients for O-O, Al-Al, and Cu-Cu collisions are studied in the color string percolation model. Our results for  $v_2$  are somewhat smaller than predicted by other groups, although with the same dependence on centrality. Our obtained  $v_3$  lie between predictions of other groups.

DOI: [10.1103/PhysRevC.103.054902](https://doi.org/10.1103/PhysRevC.103.054902)**I. INTRODUCTION**

A remarkable discovery at collider experiments has been observation of strong azimuthal correlations in heavy nuclei collisions [1–6]. It can be characterized by the nonzero flow coefficients  $v_n$  governing the correlation function of the azimuthal distribution of secondaries as

$$C(\phi) = A \left( 1 + 2 \sum_{n=1} v_n \cos(n\phi) \right). \quad (1)$$

Here

$$C(\phi) = \frac{\langle d^2\sigma/d\phi_1 d\phi_2 \rangle}{\langle d\sigma/d\phi_1 \rangle \langle d\sigma/d\phi_2 \rangle} - 1,$$

where  $\phi_{1,2}$  are azimuthal angles of the observed particles,  $\phi = \phi_1 - \phi_2$ , and  $\langle \dots \rangle$  means averaging over events.

This phenomenon can be interpreted in terms of formation of a fireball in the overlap of the colliding nuclei, consisting of the strongly interacting hot quark-gluon plasma, which subsequently freezes, hadronizes, and passes into the observed secondary hadrons. The dynamics of this transition seems to be well described in the hydrodynamical approach, which relates the final spatial anisotropy to that of the initial state.

Later a similar anisotropy was found also in collisions of smaller systems such as p-p, p-A, d-A, and He-A [7–13]. This has raised certain doubts about formation of significantly large pieces of quark-gluon plasma in the interaction region and the subsequent hydrodynamical evolution. However, calculations made within specific models [14–16] and also with the initial conditions created by gluon emission in the color glass condensate effective theory [17–19] seem to describe at least part of the experimental data quite satisfactorily. So the dynamic assumptions adopted for A-A collisions seem to work also for smaller systems.

This conclusion was earlier found in an alternative scenario for high-energy collisions, namely, the fusing color string picture. Much simpler than the hydrodynamical approach, with or without previous gluon emission in the QCD framework, it allowed a satisfactory description of the dependence of the spectra, both on the transverse momentum and angle at various energies and for various colliding particles [20]. In particular, it has been found that the fusion string model correctly describes the data on  $v_n$  in pp and AA collisions [21–23]. In this scenario the dynamics for small and large participants is qualitatively the same. The colliding nucleons form strings as soon as they are close enough, and the strings then emit the observed secondary particles. The angular anisotropy in this scenario is the result of their quenching due to the presence of the gluon field from the created strings. So essentially it is a two-stage scenario as opposed to three-stage scenarios consisting first in formation of the set of interacting nucleons, then building of the initial condition (e.g., emission of gluons) and finally the hydrodynamical expansion. Correspondingly it carries only one adjustable parameter—the universal quenching coefficient to be extracted from some data.

Remarkably, this approach does not distinguish between colliding particles of different hadronic content. In particular it has been found that it well applies not only to heavy nuclei collisions but also to p-A and d-A collisions [24]. Accordingly, in this article we apply this approach to the flow coefficients  $v_2$ ,  $v_3$  and  $v_4$  in O-O, Al-Al, and Cu-Cu collisions at 200 GeV are now planned at relativistic heavy ion collider (RHIC). We expect that our results will serve as reference points for future experimental data. Our hope is that they will describe them reasonably well.

The flow coefficients in O-O collisions have recently been studied in the approaches with either hydrodynamical evolution from the initial condition created in the color gluon condensate (CGC) framework [25,26] or with the initial parton production and the following rescattering and hadronization [a multiphase transport model (AMTP) approach, see, e.g., Ref. [27]]. Both models are much more complicated than our color string model. They distinguish the initial state formation and final state interaction. And as

Published by the American Physical Society under the terms of the [Creative Commons Attribution 4.0 International](https://creativecommons.org/licenses/by/4.0/) license. Further distribution of this work must maintain attribution to the author(s) and the published article's title, journal citation, and DOI. Funded by SCOAP<sup>3</sup>.

stated in [19], the question which of the two stages dominates in producing the final azimuthal dependence remains open. As mentioned, the color string scenario is basically much simpler than both. In this approach particle production and their azimuthal asymmetry are produced simultaneously due to the asymmetry of the created gluon field. As we shall see, it gives the flow coefficients for light nuclei on the same level and with the same centrality dependence as the two mentioned sophisticated approaches. So it seems that the complicated concrete mechanisms inherent in the latter are in fact not very essential for the final results, which apparently depend only on the overall basic dynamical structure, correctly described by the color string model.

## II. FLOW COEFFICIENTS IN THE COLOR STRING MODEL

The model was proposed a long time ago to describe multiparticle production in the soft region. Its latest development and applications are described in the review paper [20]. As mentioned in this model, particle creation and production of azimuthal asymmetry proceed simultaneously. Both are the results of the formation of the gluon field by color strings. This field, on one hand, produces particles more or less in the spirit of the Schwinger mechanism of particle creation in the external field. On the other hand, as explained below, it provides the azimuthal asymmetry due to interaction of the produced particles with the same gluon field, which by itself is azimuthal asymmetric due to the initial asymmetry of nucleons in the overlap and fluctuations.

In the model the initial strings tend to overlap and fuse into novel strings with more intrinsic color which have a higher tension and so partons with greater transverse momenta. As atomic numbers of the colliding nuclei grow, the density of strings in the transverse space grows. As a result, with the growth of their density strings fuse more intensely and this effective number grows weaker. This immediately explains the observed growth of the multiplicities in AA collisions, both with the atomic numbers and energy. Also, appearance of fused strings explains the growth of the heavy particles in these collisions. At a certain critical density clusters acquire transverse dimensions comparable to those of the interaction area (percolation), and one may consider it as formation of the drops of the quark-gluon plasma.

Particle creation in the model starts with emission of partons from the formed strings. The partons are massless quarks and antiquarks. The gluons are considered as their pairs in the approximation of a large number of colors. The partons travel in the overlap area of the colliding nuclei to hadronize into the observed particles in the end. The model does not specify the hadronization mechanism, assuming that all partons with the 100% probability transform into hadrons, which only changes the magnitude of the cross section but not its angular dependence, in the spirit of the well-known parton-hadron duality. One may think that each parton in the end picks up a soft antiparton to bleach its color (or form a finite string).

Naively one can assume that strings decay into partons ( $q\bar{q}$  pairs) by the well-known Schwinger mechanism for pair creation in a strong electromagnetic field with the

probability

$$P(p, \phi) = C_0 e^{-\frac{p_0^2}{T}}, \quad (2)$$

where  $p_0$  is the parton initial transverse momentum,  $T$  is the string tension (up to an irrelevant numerical coefficient), and  $C_0$  is the normalization factor. Distribution (2) does not depend on the azimuthal angle  $\phi$ . The string tension is determined by the magnitude of the gluon field responsible for parton creation. To extend validity of the distribution to higher momenta one may use the idea that the field and consequently string tension fluctuate, which transforms the Gaussian distribution into the thermal one [28,29]:

$$P(p, \phi) = C_1 e^{-\frac{p_0}{t}}, \quad (3)$$

with temperature  $t = \sqrt{T/2}$ .

If one allows that the emitted partons freely travel from the string to hadronize in the end the final cross section will evidently be azimuthal symmetric, since each string generates the cross section independent of the angle. To introduce the angular dependence the model assumes that the initial transverse momentum  $p_0$  of the parton is changed due to the parton interaction with the gluon field in the overlap area created by all formed strings, including the string from which the parton was emitted. So the observed particle momentum  $p$  is different from the original momentum  $p_0$ . In fact, the particle has to pass through the fused string areas and emit gluons on its way out. So in Eq. (2) or (3) one has to consider  $p_0$  as a function of  $p$  and path length  $l$  inside each string encountered on its way out:  $p_0 = f(p, l(\phi))$ , where  $\phi$  is the azimuthal angle. Since the gluon field of the strings is anisotropic due to initial anisotropy of string distribution, this quenching creates the final anisotropy and leads to nonzero flow coefficients

The radiative energy loss has been extensively studied for a parton passing through the nucleus or quark-gluon plasma as a result of multiple collisions with the medium scattering centers [30]. In our case the situation is somewhat different: the created parton moves in the external gluon field inside the string. In the crude approximation this field can be taken as being constant and orthogonal to the direction of the parton propagation. In the same spirit as taken for the mechanism of pair creation, one may assume that the reaction force due to radiation is similar to the one in the QED when a charged particle is moving in the external electromagnetic field. This force causes a loss of energy  $\epsilon$  due to photon emission, which for an ultrarelativistic particle and strong field is given by [31]

$$\frac{d\epsilon}{dt} = -\frac{8\Gamma(2/3)}{243\pi} e^2 m^2 (3\chi)^{2/3}. \quad (4)$$

Here  $\chi^2 = (e^2/m^6)(F_{\mu\nu}p_\nu)^2$ , where  $F$  is the electromagnetic field,  $p$  the momentum of the moving particle with mass  $m$  and charge  $e$ . For a situation similar to ours the field is reduced to the electric field,  $\mathbf{E}$  which is orthogonal to purely transversal  $\mathbf{p}$ . Then  $\chi = eE p_T / m^3$  and we find

$$\frac{dp_T}{dt} = -c(eE p_T)^{2/3}, \quad (5)$$

where  $c = 8\Gamma(2/3)3^{2/3}e^2/243\pi$  and is dimensionless and independent of  $m$ . The quantity  $eE$  gives the energy density along the direction of the field. For our situation it can be associated with the tension  $T$  of the string. Taking into account that for an ultrarelativistic particle  $dt = dx$  where  $x$  is the displacement along the direction, we translate Eq. (5) for our situation as

$$\frac{dp(x)}{dx} = -\kappa(T(p(x)))^{2/3}. \quad (6)$$

(We suppress the subindex  $T$  for brevity, having in mind that in other places we use exclusively the transversal momentum.) Integration of this equation in the interval  $[0, l]$  leads to our quenching formula [23]

$$p_0(p, l) = p(1 + \kappa p^{-1/3} T^{2/3} l)^3, \quad (7)$$

where  $p = p(l)$  is the final (observed) momentum and  $p_0$  is the initial one emitted from the string. The dimensionless quenching coefficient  $\kappa$  can be chosen to give the experimental values, say, for the coefficient  $v_2$  in high-energy mid-central A-A collisions, integrated over the transverse momenta.

Of course the possibility to use electrodynamic formulas for the chromodynamic case may raise certain doubts. However, in Ref. [32] it was found that at least in the  $N = 4$  SUSY Yang-Mills case, the loss of energy of a colored charge moving in the external chromodynamic field was given by essentially the same expression as in the QED.

Fusion of  $n$  strings creates new strings with a tension  $\sqrt{n}$  times greater [20]. They are unstable. So during the time elapsed while the emitted parton meets another string, the latter will be partially decayed and so have a smaller tension than at the moment of its creation. So one has to consider a nonstatic string distribution with string tensions evolving in time and gradually diminishing until strings disappear altogether. The time scale of this evolution is estimated to be considerably greater than time intervals characteristic for partons traveling inside the string matter [23]. So this effect is rather small; however, it is noticeable and can be taken into account in calculations. Effectively it only leads to a change of the value of the quenching coefficient  $\kappa$ , which in any case is to be adjusted, as explained above.

Depending on the experimental data used for this adjustment,  $\kappa$  turns out to lie in the interval  $0.5 \div 0.6$  [21,23,24,33]. In this interval the dependence of the flow coefficients on centrality and transverse momentum does not change at all, their magnitude only slightly changing by less than 5%. In this paper we adjusted  $\kappa$  to give the experimental value for  $v_2$  in mid-central Au-Au collisions at 200 GeV, integrated over the transverse momenta, which gives  $\kappa = 0.54$  [21].

Remarkably, Eq. (7) gives rise to a universal dependence of  $v_2$  on the product  $\epsilon p^{2/3} T^{1/3} l$ , where  $\epsilon$  is the eccentricity of the nuclear overlap. This scaling is well confirmed by the experimental data [6,34,35].

In the model the event is realized as a particular way the color strings are stretched between the projectile and target. Different events possess different number of strings located at different places in the overlap of the colliding nuclei. The flow coefficients can be obtained from averaging over events

of the inclusive particle distribution in the azimuthal angle for a single event (see [26]):

$$I^e(\phi) = A_0^e + 2 \sum_{n=1} (A_n^e \cos n\phi + B_n^e \sin n\phi). \quad (8)$$

The flow coefficients are then

$$v_n\{2\} = \left( \frac{\langle A_n^{e2} + B_n^{e2} \rangle}{\langle A_0^{e2} \rangle} \right)^{1/2}. \quad (9)$$

The flow coefficients for given transverse momenta  $p$  are obtained from the inclusive distribution in both  $\phi$  and  $p$ :

$$I^e(\phi, p) = A_0^e(p) + 2 \sum_{n=1} (A_n^e(p) \cos n\phi + B_n^e(p) \sin n\phi), \quad (10)$$

as

$$v_n\{2\}(p) = \frac{\langle A_n^e(p)A_n^e + B_n^e(p)B_n^e \rangle}{\langle A_0^e(p)A_0^e \rangle v_n\{2\}}, \quad (11)$$

where  $p$ -independent  $A_n, B_n$  and  $v_n\{2\}$  are the integrated quantities taken from (8) and (9).

### III. CALCULATIONS

#### A. Monte Carlo simulations

Monte Carlo simulations with the string model in principle consist, first, of distributing strings in the transverse area of the overlapping nuclei; second, in analyzing their geometrical structure and forming fused strings when they overlap; and third, studying the paths passed by the produced partons through the maze of strings to find their quenching according to Eq. (7). The actual realization of this program encounters the difficulty that the fusing strings form clusters of different forms and dimensions. Both the study of their emission and of their quenching of already emitted partons present practically unsurmountable technical problems if ones considers their exact geometries. To facilitate the problem we use a simplified approach, which was shown to give a very reasonable result as compared to the exact one [36]. Instead of clusters formed by the actual fusing of strings, we split the whole transverse area in cells having the dimension of ordinary strings ( $\sim 0.3$  fm). Distributing the strings in the area, we consider as fused the ones which get into the same cell. Then the geometry is simplified to the set of clusters represented by cells which contain fused strings made of different number of ordinary ones. Each cell cluster possesses its own string tension and emission multiplicity in accordance with the standard fusing string model. The quenching of the emitted parton is then studied in this geometry as this parton passes through different cells on its way out.

A certain problem is also in that in the simulations one has to place the colliding particles at a fixed value of the impact parameter  $b$ . However, in the experimental setup the impact parameter is not known. Instead one has to distinguish between different centralities from the observed multiplicities. So one has first to study the multiplicity at different values of  $b$ , then divide it into intervals corresponding to centralities as defined by the experimentalists, and after that study separately

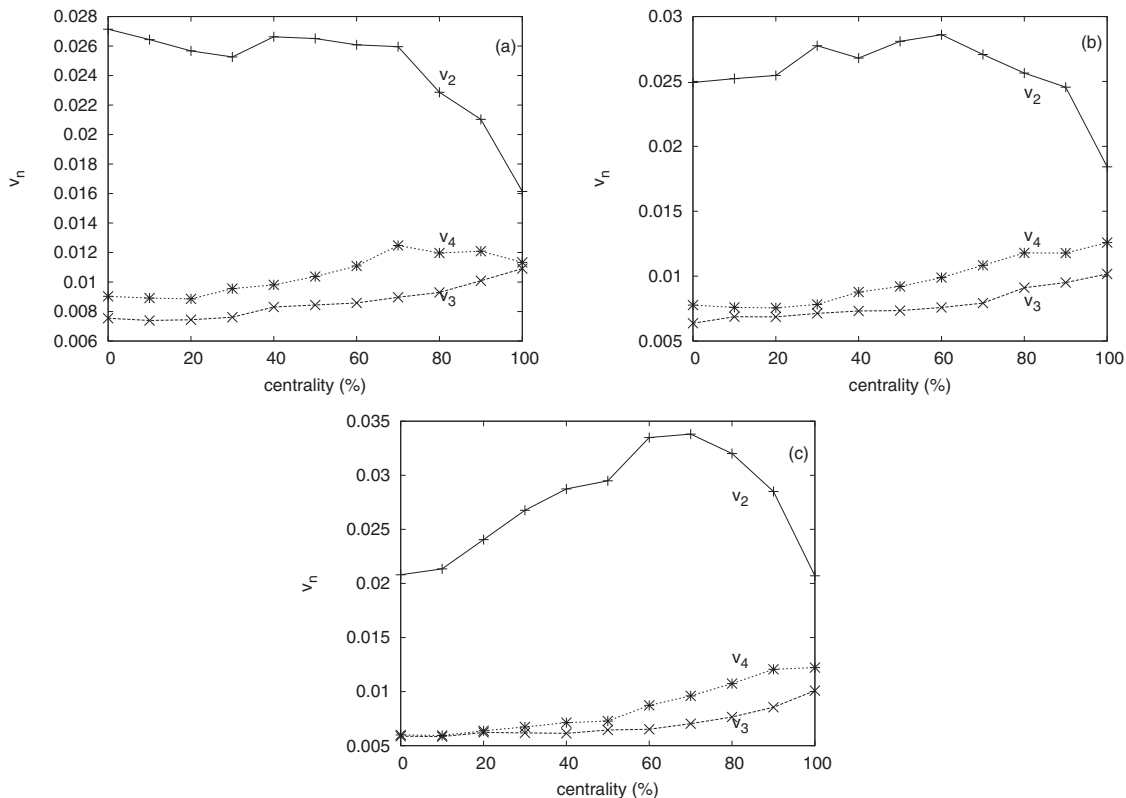


FIG. 1. The calculated flow coefficients  $v_2$ ,  $v_3$ , and  $v_4$  for O-O (a), Al-Al (b), and Cu-Cu (c) collisions at 200 GeV/c as function of centrality.

Monte Carlo simulations within a given interval of experimental multiplicities. This does not seem to present much difficulty, but to have reasonable statistics for each interval of centrality requires a considerable rise of the total number of simulations and thus of the processor time.

So our performed Monte Carlo calculations included four steps. First the transverse area was filled with interacting nucleons from both nuclei with the probability of their location determined by the appropriate transverse profile functions. Second, to each pair of interacting nucleons strings were attached. Namely, in the area space of each pair of nucleons locations of a fixed number of strings were randomly distributed with equal probability. This number for a given centrality and energy was obtained by continuation to light nuclei of the conclusions for heavier nuclei collisions in [37] for energies 62.4 and 200 GeV and in [38] for the LHC energy of 2.76 GeV. At this step all strings which were found to be located in the same cell were considered as fused (clusters), with their particular tension and multiplicity determined by the fusion mechanism [20]. At the next step one considers emission of a parton from a given string (cell). One follows the path leading from this string outside in the fixed angular direction  $\phi$ . One has to detect all the strings which the parton crosses on its way out and correspondingly find the initial momentum  $p_0$  with which the parton had started its traveling out using Eq. (7). To do this we introduced a finer division of the area in mini-cells, so as to split the cell-string area in 25 mini-cells. By following the path of the emitted parton along its way out, one determines all the mini-cells located inside

the set of strings, that is inside the occupied cells, including the cell from which the parton was emitted. The length of the path inside the encountered string determines quenching of the parton momentum according to (7) with the tension  $T$  of the string (different for different encountered ordinary or fused strings). This procedure is complicated, very consuming as to the processor time, and so strongly limits the number of simulations. The found  $p_0$  determines the probability of emission by (3). Summation over all strings gives the final inclusive cross section at a given  $\phi$ . This approach requires fixing the impact parameter to find the distribution of the colliding nucleons. So finally, to pass to the experimental observables one has to act as described above, separating the found cross section into different bins according to the values of the multiplicity, and only then perform the overall averaging.

## B. Results

Calculations were performed for O-O, Al-Al, and Cu-Cu collisions at 200 GeV/c. The reported run consists of 400 simulations divided between 11 centrality intervals from 0% to 100%. The interval of transverse momenta was taken as  $0.1 < p_T < 4$  GeV/c divided into 80 points. The interval of azimuthal angles was divided into 360 points. Our flow coefficients were calculated according to Eq. (11).

The results of calculations for  $v_2$ ,  $v_3$ , and  $v_4$  for different centralities are presented in Fig. 1 for O-O, Al-Al, and Cu-Cu collisions. In Fig. 2 we illustrate the dependence of  $v_2$ ,  $v_3$ , and

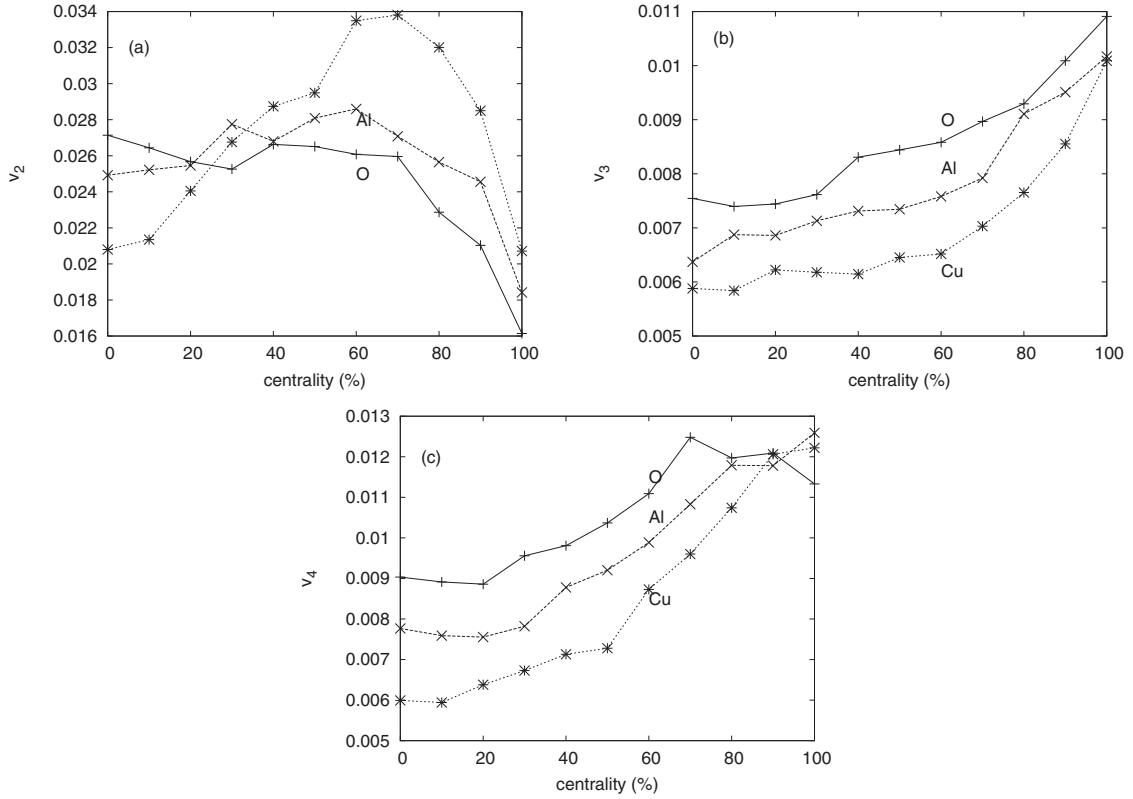


FIG. 2. The calculated flow coefficients  $v_2$  (a),  $v_3$  (b), and  $v_4$  (c) for O-O, Al-Al, and Cu-Cu collisions at 200 GeV/c as a function of centrality.

$v_4$  on the atomic numbers 16, 27, and 64 for O-O, Al-Al, and Cu-Cu collisions. In Fig. 3 we compare our calculated  $v_2$  and  $v_3$  with the predictions of [19] and [27]. Finally, we illustrate the  $p$  dependence of  $v_n$  in O-O collisions at different centralities in Fig. 4. The centrality interval in each case lies within 5% around the centrality indicated in the figures. One observes that  $v_3(p)$  turns out smaller than  $v_4(p)$  at small values of  $p$  and greater at greater values. Since the  $p$  distribution rapidly falls with  $p$ , this agrees with the relative magnitudes of the integrated  $v_3$  and  $v_4$  in Fig. 1.

Inspecting our results, we see that globally for  $v_3$  and  $v_4$  and for  $v_2$  at centralities above 30% our results have the same

pattern as for the collisions of heavier nuclei performed in the same approach [33] and reasonably agree in their behavior with the experimental data [5,6]. However, one notices a certain anomaly in the behavior of  $v_2$  at low centralities. Whereas in our earlier calculations with heavier nuclei and in the experimental data one observes a fast drop of  $v_2$  to quite small values around 1/5 of its maximal value, in our calculations this drop is much smaller for Cu-Cu and especially Al-Al collisions, and for O-O collisions we do not find any drop whatsoever. In any case, we observe a considerable rise of  $v_2$  at small centralities as compared to the heavy nuclei case. We are not sure that this behavior is not a consequence of a

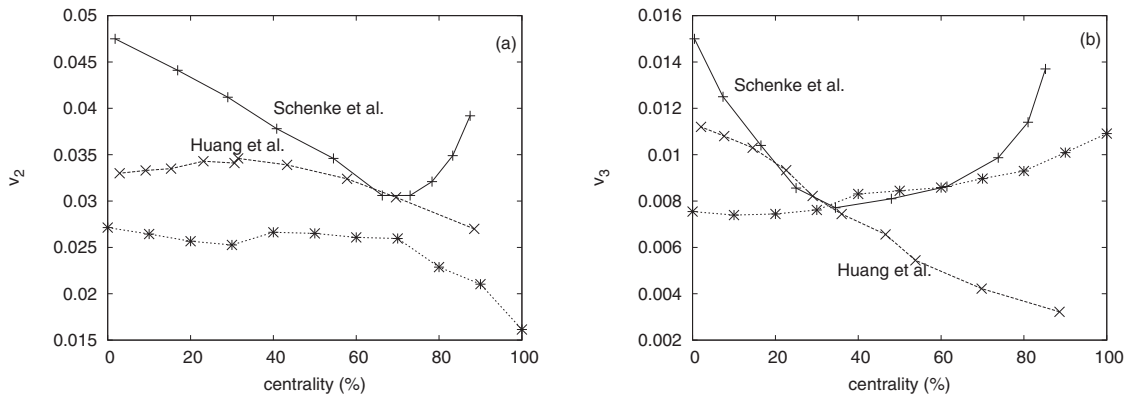


FIG. 3. The calculated flow coefficients  $v_2$  (a) and  $v_3$  (b) for O-O collisions at 200 GeV/c compared to [26] and [27].

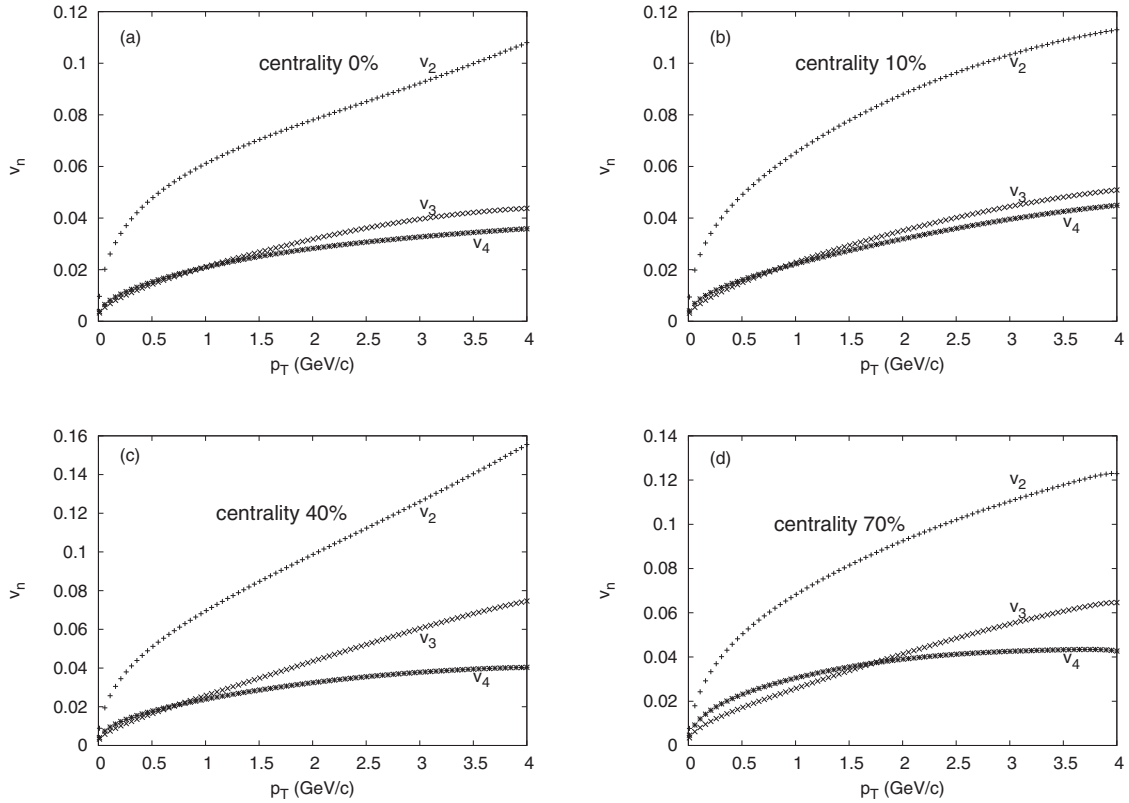


FIG. 4. The calculated flow coefficients  $v_2$ ,  $v_3$ , and  $v_4$  for O-O collisions at 200 GeV/c as a function of  $p_T$  at centralities 0 ÷ 5 (a), 10 ÷ 15 (b), 40 ÷ 45 (c), and 70 ÷ 75 (d).

too small number of events with maximal multiplicity which contributes in this region.

One has to take into account that our results were obtained by Monte Carlo simulations with a number of runs limited by our calculational possibilities to  $N_{\text{run}} = 400$ . So our curves refer only to the average values of the flow coefficients, which are known to have quite large event-to-event fluctuations [33]. An estimate of our precision can be obtained by comparing values  $\langle v^2 \rangle$  and  $\langle v \rangle^2$  found from our calculations. They give the relative error in obtained values of  $v_n$  equal to 20%. Remarkably, this figure is practically the same for all the found values of  $v_n$ , irrespective of the centrality,  $p$  dependence, and colliding nuclei. This may shift the left points for  $v_2$  in Figs. 1 and 2 down by 0.02–0.04. Still, the values of  $v_2$  at quite low centralities will remain abnormally large as compared with the situation with heavy nuclei. Remarkably, calculations of O-O collisions in Refs. [26] and [27] revealed the same peculiarity of the behavior of  $v_2$  at small centralities. Probably due to a smaller number of strings, fluctuations in their distribution become more intense, even at practically central collisions.

Due to the comparatively small statistics we do not see any reason to be concerned with details of the behavior of  $v_2$  for the different pairs of participants in Fig. 2. The obtained crossing of the curves at small centralities looks rather peculiar, but due to the mentioned statistical errors we cannot take it too seriously. Subsequent calculations with an enlarged statistics will hopefully shed some light on this point.

#### IV. DISCUSSION

Our predictions for the elliptic flow  $v_2$  are roughly of the same magnitude for O-O, Al-Al, and Cu-Cu collisions at 200 GeV showing a rather weak centrality dependence. As mentioned, at small centralities or if  $v_2$  turn out to be abnormally large, probably partially to low statistics, both triangular and quadrangular flows  $v_3$  and  $v_4$  seem to fall and rise with centrality. Remarkably, as a function of centrality, the quadrangular flow is found to be larger than the triangular one, although it is smaller as a function of  $p_T$ . Compared to the calculations of other groups, our  $v_2$  are definitely smaller than in [26] (by nearly 40%) and [27] (by  $\sim 30\%$ ), with a similar centrality dependence. As to  $v_3$ , our predictions are also smaller than in [26], with the same dependence on centrality. Compared to [27], our  $v_3$  behave differently in centrality—lower at small and higher at large centralities. One may say that on the average they are of the same magnitude. We stress that the azimuthal asymmetry in our model is directly controlled by the quenching parameter  $\kappa$  in Eq. (7). As mentioned, in these calculations it was chosen to be 0.54 from the previous similar studies of collisions on Pb at LHC. So it is trivial to raise our flows somewhat by increasing the parameter  $\kappa$ . However, this would contradict our physical picture in which  $\kappa$  is determined by the quenching of a particle passing through the gluon field independent of such external parameters as the atomic number of participants and their energy.

In conclusion, apart from the anomaly of  $v_2$  at small centralities, applied to light nuclei the fusion color string

approach seems to give results which smoothly continue earlier ones obtained for heavy nuclei. This is a natural property of the model, in which the dynamics is the same for light and heavy participants. In this respect this model does not experience problems with formation of blobs of the quark-gluon plasma (or liquid) in alternative approaches, hardly probable with light participants.

Our results are actually based on the three characteristic aspects of our model. First, it is a two-step property of the emission. The participant nucleons collide in the overlap area and then they emit strings, which are the final emitters. Second, the strings fuse into clusters with more tension, and this fusion is intensified with the growth of energy. Third is the

assumed form of the quenching in passing through the gluon fields which correspond to the formed strings. Without this quenching no azimuthal asymmetry is found in the model.

#### ACKNOWLEDGMENTS

M.A.B. appreciates the hospitality and financial support of the University of Santiago de Compostela, Spain. C.P. thanks the grant Maria de Maeztu Unit of Excellence of Spain and the support Xunta de Galicia and European Union. This work was partially done under the Project EPA 2017-83814-P of the Spanish Research State Agency, Tecnologia y Universidades of Spain.

- 
- [1] S. Afanasiev *et al.* (PHENIX Collaboration), *Phys. Rev. C* **80**, 024909 (2009).
- [2] R. Aamodt *et al.* (ALICE Collaboration), *Phys. Rev. Lett.* **107**, 032301 (2011).
- [3] A. Adare *et al.* (PHENIX Collaboration), *Phys. Rev. Lett.* **107**, 252301 (2011).
- [4] B. Alver *et al.* (PHOBOS Collaboration), *Phys. Rev. Lett.* **98**, 242302 (2007).
- [5] L. Adamczyk *et al.* (STAR Collaboration), *Phys. Rev. Lett.* **115**, 222301 (2015).
- [6] S. Acharya *et al.* (ALICE Collaboration), *J. High Energy Phys.* **07** (2018) 103.
- [7] V. Khachatryan *et al.* (CMS collaboration), *J. High Energy Phys.* **09** (2010) 091.
- [8] S. Chatrchyan *et al.* (CMS collaboration), *Phys. Lett. B* **718**, 795 (2013).
- [9] B. Abelev *et al.* (ALICE collaboration), *Phys. Lett. B* **719**, 29 (2013).
- [10] G. Aad *et al.* (ATLAS collaboration), *Phys. Rev. Lett.* **110**, 182302 (2013).
- [11] A. Adare *et al.* (PHENIX collaboration), *Phys. Rev. Lett.* **111**, 212301 (2013).
- [12] A. Adare *et al.* (PHENIX collaboration), *Phys. Rev. Lett.* **114**, 192301 (2015).
- [13] C. Aidala *et al.* (PHENIX Collaboration), *Nat. Phys.* **15**, 214 (2019).
- [14] P. Bozek, *Phys. Rev. C* **85**, 014911 (2012).
- [15] M. Habich, J. L. Nagle, and P. Romatschke, *Eur. Phys. J. C* **75**, 15 (2015).
- [16] C. Shen, J.-F. Paquet, G. S. Denicol, S. Jeon, and C. Gale, *Phys. Rev. C* **95**, 014906 (2017).
- [17] M. Mace, V. Skokov, P. Tribedy, and R. Venugopalan, *Phys. Lett.* **788**, 161 (2019).
- [18] M. Mace, V. Skokov, P. Tribedy, and R. Venugopalan, *Phys. Rev. Lett.* **121**, 052301 (2018); **123**, 039901 (2019).
- [19] B. Schenke, C. Shen, and P. Tribedy, *Phys. Lett. B* **803**, 135322 (2020).
- [20] M. A. Braun, J. Dias de Deus, A. S. Hirsch, C. Pajares, R. P. Scharenberg, and B. K. Srivastava, *Phys. Rep.* **599**, 1 (2015).
- [21] M. A. Braun and C. Pajares, *Eur. Phys. J. A* **54**, 185 (2018).
- [22] I. Bautista, L. Cuqueiro, J. Dias de Deus, and C. Pajares, *J. Phys. G* **37**, 015103 (2010).
- [23] M. A. Braun, C. Pajares, and V. V. Vechernin, *Nucl. Phys. A* **906**, 14 (2013).
- [24] M. A. Braun and C. Pajares, *Eur. Phys. J. A* **56**, 41 (2020).
- [25] B. Schenke, C. Shen, and P. Tribedy, *Nucl. Phys. A* **1005**, 121756 (2020).
- [26] B. Schenke, C. Shen, and P. Tribedy, *Phys. Rev. C* **102**, 044905 (2020).
- [27] S. Huang, Z. Chen, W. Li, and J. Jia, *Phys. Rev. C* **101**, 021901 (2020).
- [28] A. Bialas, *Phys. Lett. B* **466**, 301 (1999).
- [29] J. Dias de Deus and C. Pajares, *Phys. Lett. B* **642**, 455 (2006).
- [30] R. Baier, Y. I. Dokshitzer, A. H. Mueller, S. Peigne, and D. Schiff, *Nucl. Phys. B* **483**, 201 (1997); **484**, 265 (1997).
- [31] V. I. Ritus and A. I. Nikishov, *Sov. Phys. JETP* **19**, 529 (1964).
- [32] A. Mikhailov, [arXiv:hep-th/0305196](https://arxiv.org/abs/hep-th/0305196).
- [33] M. A. Braun, C. Pajares, and V. V. Vechernin, *Eur. Phys. J. A* **51**, 44 (2015).
- [34] C. Andres, J. Dias de Deus, A. Moscoso, C. Pajares, and C. Salgado, *Phys. Rev. C* **92**, 034901 (2015).
- [35] C. Andres, M. A. Braun, and C. Pajares, *Eur. Phys. J. A* **53**, 41 (2017).
- [36] M. A. Braun, R. S. Kolevov, C. Pajares, and V. V. Vechernin, *Eur. Phys. J. C* **32**, 535 (2004).
- [37] T. J. Tarnowsky, B. K. Srivastava, and R. P. Scharenberg (for the STAR Collaboration), *NuKleonika* **51S3**, S109 (2006).
- [38] J. Dias de Deus, A. S. Hirsch, C. Pajares, R. P. Scharenberg, and B. K. Srivastava, *Eur. Phys. J. C* **72**, 2123 (2012).